JCTC Journal of Chemical Theory and Computation

Article

pubs.acs.org/JCTC

Assessment of a Nonlocal Correction Scheme to Semilocal Density Functional Theory Methods

Andreas Heßelmann*

Lehrstuhl für Theoretische Chemie, Universität Erlangen-Nürnberg, Egerlandstr. 3, D-91058 Erlangen, Germany

Supporting Information

ABSTRACT: A nonlocal correction method to (semi)local density-functional theory (DFT) methods is derived that is based on a partitioning of the correlation-energy density into atom−atom contributions. Nonlocal interaction contributions, which are absent in standard DFT methods, are introduced in this method by using atomic weight functions that do not vanish exponentially as the atomic densities but with the inverse sixth power of the atomic distances. The parameters contained in these weight functions were fitted to reproduce intermolecular interaction energies for a range a small dimer systems. The new functional has then been tested both for intermolecular interactions, using the S22, S66 × 8, and IonHB databases from Hobza et al., and for other thermodynamical properties using a subset of 14 databases of the GMTKN30 database of Grimme et al. It is found that for intermolecular interactions the accuracy of the method is often higher than with standard DFT+D methods while for other properties, such as reaction energies or relative conformation energies of medium sized organic molecules, the accuracy is similar to hybrid-DFT+D methods. The nonlocal correction method has been tested also to predict the interaction energy of the water−graphene system yielding an estimated interaction energy of −2.87 kcal/mol, which is in line with previous theoretical investigations.

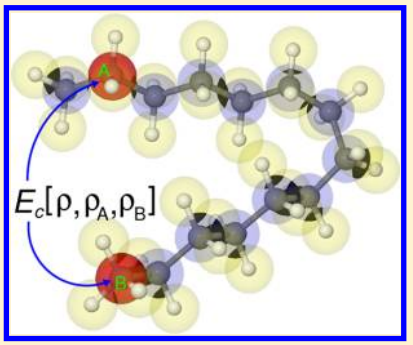

1. INTRODUCTION

In recent years, there has been a very active research in the development of new density functional theory (DFT) methods[1] that either explicitly incorporate or mimic the important long-range correlation interactions between molecules that can not be described with standard exchange-correlation (xc) functionals of the local density approximation (LDA) or the generalized gradient approximation (GGA) type.[2] Roughly these methods can be classified into (1) methods that directly improve DFT functionals to describe long-range correlation interactions and (2) methods that add a separate dispersion contribution to the DFT energy that is damped at short interatomic distances.

Methods that belong to the first type are more within the realm of DFT because they define, in addition to a density functional, a corresponding corrected xc potential and higher order derivatives that affect also the calculation of molecular properties. Examples of these methods are the highly parametrized meta- and hybrid-GGA functionals developed by Zhao and Truhlar,[3−6] which have been applied with some success for the description of weakly interacting systems.[7,8] However, these functionals can only improve the medium-range correlation contributions to the interaction energy; they lack the ability to describe the long-range correlation interaction qualitatively correct. Moreover, both the use of highly parametrized functionals including many terms in a power series expansion and the inclusion of kinetic energy-density terms in the functional can lead to numerical instabilities that can cause unphysical intermolecular potentials.[9] Another approach to explicitly describe long-range correlation interactions via a density functional are the nonlocal, so-called van-der-Waals density functionals (vdW-DF) originally derived by Langreth et al.[10−15] In these methods, the nonlocal origin of the long-range correlation interaction is explicitly incorporated via a nonlocal correlation kernel in a double-space integral, see refs 10−12. It should be noted that this kernel function in all current versions of the vdW-DF type functionals is damped for short interelectronic distances, and more short-range correlation contributions are described with a standard LDA- or GGA-type functional. This damping in vdW-DF functionals clearly differs from the damping used in DFT+D methods (see below) because in the latter the damping depends on the atomic distances while in the former a single damping parameter is used that depends on the interelectronic distance. Nevertheless, in both cases, the damping serves for the same purpose, namely to ensure finiteness of the long-range correlation contribution and to avoid the problem of double counting of electron correlation effects. In the VV10 functional of Vydrov et al., for example, the damping parameter was fitted to reproduce the CCSD(T) interaction energies for the S22 set[16] of dimers.[15] In this sense, the vdW-DF's are related to the second class of methods in which an extra dispersion energy contribution is added to existing standard DFT functionals. A recent variant of the vdW-DF, termed as VV10 has been shown to yield fairly well intermolecular interaction energies.[15]

The currently most popular and historically oldest DFT approaches that include long-range interactions are the DFT+D

Received: August 24, 2012

   dx.doi.org/10.1021/ct300735g | J. Chem. Theory Comput. XXXX, XXX, XXX−XXX

methods in which the dispersion interaction contribution is calculated from atom−atom dispersion contributions that are added to the DFT energy calculated using standard functionals.[17−20] Because of this, the long-range contribution in these methods needs to be damped at short interatomic distances, both to ensure finiteness and to avoid the double-counting of correlation effects in the medium-range. While the earliest versions of this approach used atomic dispersion coefficients that were fitted to reproduce molecular C_6 values, binding energies, and bond distances of (usually) small molecular systems,[17,18,21] in the more recent versions, they are calculated by using more sophisticated approaches. For example, in the D3 correction method by Grimme, the atom−atom dispersion interaction contributions are calculated from frequency-dependent polarizabilities calculated for corresponding hydrid molecules of the two corresponding atoms.[20] In the method of Tkatchenko et al., the interatomic dispersion coefficients are derived from the electron density of a molecule or solid accompanied by accurate reference data for the free atoms.[22,23] The local response dispersion (LRD) method of Sato and Nakai uses a simple model of the density−density response function for the homogeneous electron gas that enables the calculation of localized polarizabilities that in turn are used as input for the calculation of atom−atom dispersion coefficients.[24] Finally, a number of methods have been developed that are related to the exchange-hole dipole moment (XDM) model by Becke and Johnson[25−27] in which the long-range atom−atom contributions to the correlation energy are explictly dependent on either the electron density[27−29] or the Kohn−Sham orbitals.[30]

A third type of approach that differs from the ones described above is the DCACP (dispersion-corrected atom centered core potential) method by Röthlisberger et al.[31,32] In this method, the long-range correlation correction is indirectly modeled through properly optimized atom-centered nonlocal potentials that are normally used in the context of pseudopotentials for core electrons. A DCACP corrected BLYP functional has been tested for the JSCH-2005 database which contains interaction energies for biomolecules.[33] It has been shown that this method yields a mean unsigned error of 1.6 kcal/mol to accurate ab initio reference results for these complexes. A disadvantage of the DCACP method is, however, that it can not reproduce in general the correct asymptotic $1/R^6$ behavior of the correlation energy as can be observed in potential energy curves of the rare gas dimers[32] or the stacked benzene dimer.[34] Moreover, at present, it is not clear whether the core potentials used in the DCACP method are able to reflect the changes of dispersion coefficients with the hybridization or oxidation state of an atom in a molecule or solid. For example, the DCACP interaction energies between hydrocarbons composed of sp^3, sp^2, and sp hybridized carbon atoms reveals that the ethane dimer is underbound by about 26% while the corresponding ethene and ethyne dimer interaction energies are close to reference values.[35]

In this work, a conceptually new approach has been developed and tested that directly modifies existing DFT functionals in order to account for long-range correlation energies and thus can be classified as belonging to the first group of methods of the list given above. This is achieved by partitioning the correlation-energy density into atom−atom contributions using a double Hirshfeld partitioning of the molecular volume. The correct long-range behavior of the intermolecular correlation energy is then obtained by using different weight functions for the same-atom and different-atom contributions to the correlation energy. A detailed description of this method is given in section 2. Section 3 describes the technical details of the calculations that have been performed. In section 4, the performance of the approach is tested for describing intermolecular interaction energies (subsection 4.1), general thermochemical and kinetic properties (subsection 4.2), and, in particular, the interaction between a water molecule with a graphene surface as a case study (subsection 4.4). In section 4.3, the dependence of the atom−atom contribution to the intermolecular correlation energy on the hybridization and oxidation state is analyzed. Finally, section 5 summarizes the results.

2. METHOD

In standard density functional theory (DFT) methods the exchange-correlation (xc) contribution to the total energy is calculated as

$$E_{xc}[\rho] = -c\int d\mathbf{r}\,\rho^{4/3}(\mathbf{r})f(\rho, \nabla\rho, \nabla^2\rho, ...) = -c\int d\mathbf{r}\, z(\rho, \nabla\rho, \nabla^2\rho, ...) \quad (1)$$

where c is a constant, ρ is the electronic energy, and $\nabla\rho, \nabla^2\rho$, ... are its derivatives. The function f depends on the density and its derivatives. In the most common (exchange part of the) local density approximation (LDA), density variations are neglected and the function f is set equal to one and the constant $c^{LDA} = {}^3/_4\,({}^3/_\pi)^{1/3}$. DFT methods taking into account also density derivatives, so-called generalized gradient approximation (GGA) functionals, can be termed as semilocal functionals, because they still depend locally on the density and its derivatives but, in contrast to LDA, can better describe situations in which the density undergoes rapid changes as in molecules.

It is clear from the above formulation that neither the LDA nor the GGA approach are able to describe long-range correlation interactions (also termed dispersion or van der Waals interactions) between molecules, which at large distances R_{AB} between the molecules A and B can be described by the asymptotic expansion (neglecting anisotropies of the molecular polarizabilities)

$$E_c^{longrange}(R_{AB}) = -\frac{C_6}{R_{AB}^6} - \frac{C_8}{R_{AB}^8} - ... \quad (2)$$

where C_6, C_8, ... are the leading-order dispersion coefficients of the supersystem AB. To correct this deficiency of standard DFT methods, in this work, the correlation contribution to the xc functional (most DFT functionals, such as LDA, PBE, and BLYP, are partitioned into an exchange and a correlation functional) is partitioned into atomic (local) and interatomic (nonlocal) terms using a double Hirshfeld partitioning:

dx.doi.org/10.1021/ct300735g | J. Chem. Theory Comput. XXXX, XXX, XXX−XXX

$$E_c^{DFT}[\rho] = \int d\mathbf{r} \sum_A^N \sum_B^N w_A(\mathbf{r}) w_B(\mathbf{r}) z(\rho, \nabla\rho, \nabla^2\rho, ...)$$
$$= \sum_A^N \int d\mathbf{r}\, w_A^2(\mathbf{r}) z(\rho, \nabla\rho, ...) + 2 \sum_A^N \sum_{B<A}^N \int d\mathbf{r}\, w_A(\mathbf{r}) w_B(\mathbf{r}) z(\rho, \nabla\rho, ...)$$
$$= E_c^{local}[\rho] + E_c^{nonlocal}[\rho] \quad (3)$$

where A,B are atomic indices and N is the total number of atoms in the molecular system. The atom-centered weight functions w_A are defined as

$$w_A(\mathbf{r}) = \frac{\rho_A(\mathbf{r})}{\sum_A \rho_A(\mathbf{r})} = \frac{\rho_A(\mathbf{r})}{\rho_{tot}(\mathbf{r})} \quad (4)$$

with ρ_A corresponding to spherical atomic densities. In this work, they are approximated by spherical Slater densities determined using Slater's rules, see ref 36. Note that from eq 4 it follows that $\sum_{A,B}^N w_A(r) w_B(r) = 1$, so that using the partitioning of eq 3 the total correlation energy is unaffected.

The main idea of this work now arises from the observation that an atom−atom contribution to the nonlocal term $E_c^{nonlocal}$ in eq 3 decreases exponentially with an increasing atom−atom distance, since the overlap between w_A and w_B decays exponentially and the function z has the form of eq 1. In an alternative partitioning of E_c^{DFT}, the correlation energy may be written as

$$E_c^{DFT}[\rho] = \sum_A^N \int d\mathbf{r}\, \tilde{w}_A^2(\mathbf{r}) z(\rho, \nabla\rho, ...) + 2 \sum_A^N \sum_{B<A}^N \int d\mathbf{r}\, \tilde{w}_A(\mathbf{r}) \tilde{w}_B(\mathbf{r}) z(\rho, \nabla\rho, ...) \quad (5)$$

with the modified weight functions $\tilde{w}_A = \tilde{\rho}_A/\tilde{\rho}_{tot}$ chosen such that the overlap $\int d\mathbf{r}\, \tilde{\rho}_A(\mathbf{r})\, \tilde{\rho}_B(\mathbf{r})$ does not vanish exponentially but only as $1/R_{AB}^6$ with increasing distance R_{AB} of the atomic centers. It can be shown that with this modification also any integral $\int dr\, w_A(r) w_B(r)\, g(r)$ with a function g having the property $\int d\mathbf{r}\, g(\mathbf{r}) \underset{R_{AB}\to\infty}{\ll} 1/R_{AB}^6$ will decay as $1/R_{AB}^6$ when $R_{AB} \to \infty$. Thus, to correct the deficiencies of E_c^{DFT} to describe long-range correlation effects, the following modification to eq 3 is proposed:

$$E_c^{DFT(NL)}[\rho] = \sum_A^N \int d\mathbf{r}\, w_A^2(\mathbf{r}) z(\rho, \nabla\rho, ...) + 2 \sum_A^N \sum_{B<A}^N \int d\mathbf{r}\, \tilde{w}_A(\mathbf{r}) \tilde{w}_B(\mathbf{r}) z(\rho, \nabla\rho, ...) \quad (6)$$

that is, the local DFT part remains unaffected by the new partitioning while the nonlocal part is calculated using the modified weight functions $\tilde{w}_A$. In contrast to the commonly applied dispersion corrections to DFT that use damped atom−atom dispersion interaction terms (DFT+D methods) that are added to the total xc energy, this new approach is an implicit improvement to the DFT functional. As such, the above partitioning also defines a modified xc potential through the derivatives

$$\frac{\widetilde{\partial z}}{\partial x} = \left(\sum_A^N w_A^2(\mathbf{r}) + \sum_A^N \sum_B^N \tilde{w}_A(\mathbf{r}) \tilde{w}_B(\mathbf{r}) \right) \frac{\partial z}{\partial x}$$
$$x = \{\rho, \nabla\rho, ...\} \quad (7)$$

Therefore, the long-range correlation correction also affects the Kohn−Sham orbitals and eigenvalues.

The question is now how to choose the modified weight functions $\tilde{w}_A$ or the modified densities $\tilde{\rho}_A$. Other than in DFT+D methods, there is no possilbility to estimate their asymptotic form, as they can not directly be related to atomic multipoles. On the other hand it appears to be reasonable to set $\tilde{\rho}_A \approx \rho_A$ for small distances from the atomic nucleus and to use the normalization constraint $\int d\mathbf{r}\, \tilde{\rho}_A(\mathbf{r}) = \int d\mathbf{r}\, \rho_A(\mathbf{r}) = N_{elec}$ where N_{elec} is the number of electrons of the corresponding atom. In this work these conditions are fulfilled by using

$$\tilde{\rho}_A(\mathbf{r}) = \mathcal{N}\left(\rho_A(\mathbf{r}) + f(r, p_1) \frac{p_2}{r^6} \right) = \mathcal{N}\left(\rho_A(\mathbf{r}) + \left(\frac{1}{2}[\mathrm{erf}(r + p_1) + \mathrm{erf}(r - p_1)] \right)^6 \frac{p_2}{r^6} \right) \quad (8)$$

where r denotes the distance from the atomic nucleus, $\mathcal{N}$ is a normalization constant to ensure that $\int d\mathbf{r}\, \tilde{\rho}_A(\mathbf{r}) = N_{elec}$ and p_1 and p_2 are empirical parameters. The function $f(r,p_1)$ can be interpreted as a damping function that goes to zero for $r \to 0$ and to 1 as r increases. Thus, after normalization, it has the effect that it shifts charge from the inner to the outer region.

The main problem of the approach described above is how to choose the parameters p_1 and p_2 in eq 8. As already stated, there is no direct link to physical properties of the atoms. Moreover, this problem is inevitably connected with the underlying density functional chosen. Here the PBE = PBEx + PBEc (PBE exchange+correlation) functional of Perdew, Burke, and Ernzerhof has been used.[37] However, in contrast to the original PBEx functional, the parameter κ that is equal to 0.804 in the original functional has been modified to a value 0.9. The reason for this modification, similar to the method of ref 30, was that using the standard PBE functional an additional long-range correlation correction often leads to a considerable overestimation of interaction energies for dimers dominated by electrostatic interactions. The modified PBE functional with κ = 0.9 is termed modPBE in this work. The parameters p_1 and p_2 were then determined by optimizing the intermolecular interaction energies for a set of dimer systems to accurate (complete basis set) CCSD(T) reference results. The set of dimer systems chosen were $(CH_4)_2$, $(C_2H_4)_2$, C_2H_4−C_2H_2, benzene$_2$(PD) using the structures from the S22 database[16] and, in addition, a set of hydrogen-bridged dimers containing hydrides of the atoms N, O, F ,Si, P, S, Cl from the second and third row (structures were optimized using MP2 in the aug-cc-pVTZ basis set). It was found that the parameter p_1 can be set globally to the value p_1 = 4.0 a_0. Concerning the parameter p_2, however, it was found that a much better agreement with reference interaction energies is obtained if it has individual values for a given atom. The optimized values used in this work, yielding a mean absolute error of 0.25 kcal/mol of the interaction energies for the fitting set, are given in Table 1.

dx.doi.org/10.1021/ct300735g | J. Chem. Theory Comput. XXXX, XXX, XXX−XXX

Table 1. Atomic Parameters p_2 (eq 8) Used in This Work (Values in au)

atom	p_2
H	2.0
C, Si	7.0
N, P	6.0
O, S	5.0
F, Cl	4.0

In summary, the total xc energy of the new approach is calculated by the sum

$$E_{xc}^{\mathrm{modPBE(NL)}} = E_x^{\mathrm{PBEx}}(\kappa = 0.9) + E_c^{\mathrm{PBEc(NL)}} \quad (9)$$

where the correlation contribution $E_c^{\mathrm{PBEc(NL)}}$ is calculated from eq 6 using the modified weight functions as described above.

3. TECHNICAL DETAILS

The nonlocal correction scheme to DFT (termed DFT(NL) hereafter) described in section 2 has been tested for a number of benchmark databases, namely S22,[16] S66 × 8,[38] IonHB,[39] and 14 subsets of the GMTKN30 database.[40−42] The S22, S66 × 8, and IonHB databases have been developed by Hobza and co-workers and contain noncovalently bound dimers in their equilibrium structure (S22), and neutral (S66 × 8), and ionic (IonHB) dimer systems also at nonequilibrium geometries, see refs 16, 38, and 39 for details. From the GMTKN30 database, developed by Grimme et al.,[40] the following subsets were chosen: BHPERI (barrier heights of pericyclic reactions), ISO34 and ISOL22 (isomerization energies of small, medium-sized and large organic molecules), DC9 (a database containing nine difficult cases for DFT), DARC (Diels−Alder reaction energies), BSR36 (bond separation reactions of saturated hydrocarbons), IDISP (intramolecular dispersion interactions), WATER27 (binding energies of water, $H^+(H_2O)_n$ and $OH^-(H_2O)_n$ clusters), S22 (see above), ADIM6 (interaction energies of *n*-alkane dimers), and the PCONF, ACONF, SCONF, and CYCONF databases (containing systems to study the performance for predicting relative energies of tripeptide, alkane, sugar, and cysteine conformers). The geometries and all reference data were taken from ref 43 (S22, S66 × 8, IonHB) and ref 42 (GMTKN30), with exception of the CCSD(T) reference data for the S22 database, which were taken from ref 44.

The DFT(NL) method has also been applied to study the interaction energy of water−acene (acene = benzene, coronene, dodecabenzocoronene (DBC), circum-DBC (cDBC), and circum-cDBC (ccDBC)) complexes in order to estimate the interaction energy of a water molecule with graphene. Two different structures have been used, one in which only one hydrogen atom interacts with the π-system of the acene surface (Figure 5a) and one in which both hydrogen atoms point toward the acene surface (Figure 5b). These structures were taken from two recent works of Jenness and Jordan[45,46] and have been optimized using MP2 in case of the first structure and the DFT-SAPT method in case of the second structure, see refs 45 and 46 for details. To extrapolate the water−acene interaction energies to those of the water−graphene system, the noncharge-penetration contribution to the electrostatic interaction energy of water−acene and water−graphene systems was calculated using the Orient4.7 program by Stone.[47] For this, the distributed multipoles up to a rank of $l = 5$ were calculated from the DFT densities of the water and the acene molecules using cutoffs of 0.65 Å for carbon and 0.35 Å for hydrogen employing the DMA (distributed multipole analysis) program by Stone.[48] For graphene, as explained in ref 45, only the multipoles $Q20$, $Q33s$, $Q40$, and $Q53s$ of the carbon atom remain nonzero compared to the acene molecules (the acene molecules were oriented perpendicular to the *z*-axis with the center of the coordinate system located in the center of the inner carbon ring and two carbon atoms of the inner ring placed on the *y*-axis). These were approximated using the corresponding multipoles for the inner carbon atoms of the cDBC molecule. The noncharge-penetration contribution to the electrostatic interaction energy could then be extrapolated using the difference between the electrostatic interaction energy of cDBC-H_2O and graphene-H_2O.

All calculations were done using the def2-QZVP basis set,[49,50] which contains semidiffuse functions and thus avoids linear dependencies in case of large molecules. For systems containing 300 basis functions and more density-fitting of the Coulomb contribution to the Kohn−Sham matrix has been used using the corresponding def2-QZVP-JFit fitting basis set.[51] In case of the WATER27 database, it has been observed that the omission of diffuse functions leads to a relatively large basis set superposition error (BSSE) for the larger complexes. Therefore, in this case, the augmented def2-aQZVP orbital and fitting basis sets were used. In all other benchmark systems for studying intermolecular interactions (S22, S66 × 8, IonHB, ADIM6) and in the calculations of the water−acene interaction energies, the BSSE has been reduced using the Boys−Bernadi counterpoise correction.[52] For the water−acene systems the def2-SVP, def2-TZVP,[50] and def2-QZVP orbital and Coulomb-fitting basis sets were used.

All calculations were performed using the *MOLPRO* quantum chemistry program.[53]

4. RESULTS

4.1. Intermolecular Interaction Energies. Table 2 shows the interaction energies for the modPBE and modPBE(NL) functionals for the S22 database along with extrapolated second-order Møller−Plesset (MP2) and coupled-cluster singles doubles with perturbative triples (CCSD(T)) reference results taken from ref 44. It can be observed that the deviations of the modPBE interaction energies to those of CCSD(T) are unacceptably large, especially for the dispersion dominated complexes, for which a mean absolute error (mae) of over 5 kcal/mol is obtained. This is strongly improved by using the corrected modPBE(NL) functional, which performs only slightly worse than MP2 for the hydrogen-bridged systems but clearly improves upon MP2 for the dispersion dominated and mixed-type sytems if compared to CCSD(T) interaction energies. The mean absolute error of modPBE(NL) for the 22 dimer system is only 0.20 kcal/mol, which is lower than measured with any DFT-D3 method (DFT method containing the D3 correction by Grimme[20]) used in the benchmark of ref 40; see also ref 42 for comparison. In another recent benchmark of Marom et al. that studies the performance of the Tkatchenchko-Scheffler[22] van-der-Waals correction (TS-vdW) to DFT methods, only the TPSS(TS-vdW) functional yields about the same accuracy for the S22 database as the modPBE(NL) functional of this work.[23] Compared to this, the most recent nonlocal vdW-DF functional from Vydrov and Voorhis, termed as VV10, performs worse for the S22 benchmark system having a mean absolute error of 0.31 kcal/mol; see ref 15.

dx.doi.org/10.1021/ct300735g | J. Chem. Theory Comput. XXXX, XXX, XXX−XXX

Table 2. Intermolecular Interaction Energies for the S22 Complexes (in kcal/mol)[a]

dimer	MP2/cbs	CCSD(T)/cbs	modPBE	modPBE(NL)
$(NH_3)_2$ (C_{2h})	−3.16	−3.17	−2.53	−3.18
$(H_2O)_2$ (C_s)	−4.98	−5.02	−4.57	−5.02
$(HCOOH)_2$ (C_{2h})	−18.57	−18.80	−17.21	−19.00
$(CHONH_2)_2$	−15.84	−16.12	−13.89	−15.82
uracil−uracil (C_{2h})	−20.41	−20.69	−17.58	−20.11
2-pyridoxine−2-aminopyridine	−17.37	−17.00	−14.41	−17.27
AT (WC)	−16.54	−16.74	−13.36	−16.61
mae	0.20		2.00	0.22
|Δ| [%]	1.26		14.57	1.24
$(CH_4)_2$ (D_{3d})	−0.49	−0.53	0.04	−0.60
$(C_2H_4)_2$ (D_{2d})	−1.58	−1.50	0.02	−1.35
Bz−CH_4 (C_3)	−1.81	−1.45	0.26	−1.40
Bz−Bz (C_{2h})	−4.96	−2.62	2.59	−2.68
pyrazine−pyrazine (C_s)	−6.91	−4.20	1.52	−4.28
uracil−uracil (C_2)	−11.10	−9.74	−1.59	−9.87
indole−Bz (stacked)	−8.09	−4.59	3.24	−4.49
AT (stacked)	−14.83	−11.66	0.23	−11.56
mae	1.70		5.32	0.09
|Δ| [%]	38.62		127.19	4.48
C_2H_4−C_2H_2 (C_{2v})	−1.67	−1.51	−1.00	−1.68
Bz−H_2O (C_s)	−3.54	−3.29	−1.64	−3.27
Bz−NH_3 (C_s)	−2.66	−2.32	−0.59	−2.24
Bz−HCN (C_s)	−5.16	−4.55	−2.41	−4.36
Bz−Bz (C_{2v})	−3.63	−2.71	−0.33	−2.34
indole−Bz (T-shaped)	−6.98	−5.62	−1.42	−5.06
phenole−phenole	−7.76	−7.09	−3.16	−6.26
mae	0.61		2.46	0.32
|Δ| [%]	16.24		63.99	7.87
mae (total)	0.88		3.35	0.20
|Δ| [%] (total)	19.61		71.25	4.53

[a]The mean absolute errors (mae) and relative deviations (|Δ|) to the CCSD(T) reference values are shown for each group of complexes (hydrogen bonded: top, dispersion dominated: middle and mixed-type: bottom). The last two lines show the total mean absolute errors and total relative deviations, respectively. The basis set extrapolated MP2 and CCSD(T) values are taken from ref 44.

To study the performance of the modPBE(NL) functional also at nonequilibrium structures of intermolecular complexes, the S66 × 8 and IonHB databases of Hobza et al. were chosen which, in addition to the respective equilibrium structures, contain two structures at shorter and five structures at longer distances of the monomers for each complex. Figure 1 shows the mean absolute errors of the modPBE(NL) functional to the extrapolated CCSD(T) interaction energies of the S66 × 8 database for all 66 complexes (Figure 1a) as well as separately for the hydrogen-bridged, dispersion dominated, and mixed-type complexes (Figure 1b−d). As expected, in the short-range repulsive region, the modPBE(NL) interaction energies show the largest absolute errors that, however, do not exceed 0.5 and 0.3 kcal/mol at scaled distances of 0.90 and 0.95, respectively. At distances of 1.00 to 1.25, the errors of the modPBE(NL) interaction energies are roughly the same and amount to 0.20 kcal/mol on average. The smallest absolute errors are found for the large distance structures, clearly due to the small total interaction energies for these distances. A comparison of the diagrams in Figure 1b−d shows that, in contrast to MP2, the errors of the modPBE(NL) interaction energies depend very little on the type of complex: the total mae for the hydrogen-bridged systems is 0.18 kcal/mol, while for the dispersion dominated and mixed-type systems a total mae of 0.17 kcal/mol is obtained. For comparison, note that in a recent study of the performace of DFT-D3 methods for the S66 × 8 database by Grimme the smallest total error was found for the BLYP-D3 method amounting to 0.24 kcal/mol.[54]

Larger errors of 0.5 kcal/mol on average of the interaction energies of modPBE(NL) are found for the ionic hydrogen-bridged systems of the IonHB database, see Figure 2. While this error is similar to the one obtained by the BLYP-D3 functional,[39] it likely is related to the fact that the interaction of charged molecules is more difficult to describe by GGA-type functionals due to charge-transfer contributions that are not well described by local exchange functionals.

All interaction energies for the S66 × 8 and IonHB databases are compiled in the Supporting Information.

4.2. Performance for 14 Subsets of the GMTKN30 Database. The mean absolute errors to accurate reference results (mostly extrapolated CCSD(T) values) of the modPBE-(NL) functional for each individual subset of the 14 subsets of the GMTKN30 database (see section 3) are shown in Figures 1−3 in the Supporting Information. These contain also the errors of DFT methods including damped dispersion corrections for comparison. Here, only the overall performance is analyzed and compared to other methods by using a weighted mean absolute error for all 14 databases. This is calculated from the formula

$$\text{wmae} = \frac{1}{N}\sum_{i=1}^{\text{database}} \frac{\text{mae}_i}{|\Delta E^{\text{av}}|_i} \tag{10}$$

with $N(=14)$ being the number of different databases, mae_i being the mean absolute error for database labeled i and $|\Delta E^{\text{av}}|_i$ corresponds to the average absolute energy of the respective database taken from ref 40. The result is shown in the diagram in Figure 3, which also shows the wmae's for some second-order perturbation theory based wave function methods (WF) and GGA, meta-, hybrid, and double-hybrid functionals with and without the D3 dispersion correction of Grimme. These numbers are based on an average of the wmae's for the range of methods reported on the GMTKN30 Web site.[42] The diagram in Figure 3 shows that both with the D3-dispersion correction and with the nonlocal correlation correction (NL) used in this work the accuracy of the respective method is significantly improved; for example, for GGA-type functionals, the wmae decreases by over 5 units using the D3 or NL correction. In case of the modPBE(NL) method of this work the wmae is about 2.5, which is clearly better than the average errors of the GGA-D3 and meta-GGA-D3 methods and comparable to the errors of the computationally more expensive (double-)hybrid-D3 and WF methods. This shows that the NL correction not only leads to improvements for the description of intermolecular interaction energies (see section 4.1) but also yields a reasonable description of other properties, namely thermochemical or kinetic properties; see section 3 and the Supporting Information.

4.3. Dependence of Atom−Atom Correlation Contribution to the Interaction Energy on Hybridization and Oxidation State. It is well-known that the dispersion

dx.doi.org/10.1021/ct300735g | J. Chem. Theory Comput. XXXX, XXX, XXX−XXX

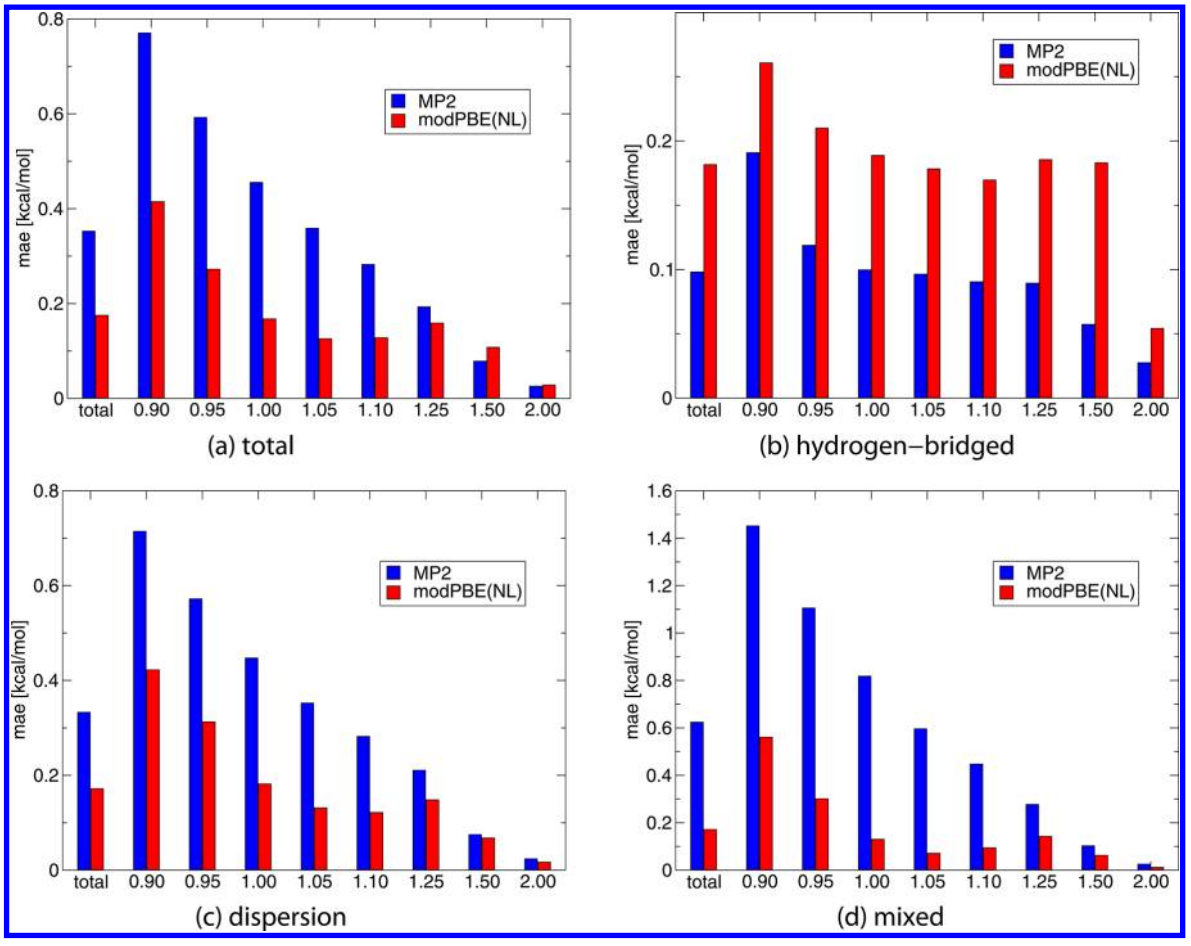

Figure 1. S66 × 8 database: mean absolute errors of MP2/cbs and modPBE(NL) interaction energies to extrapolated CCSD(T) values. The numbers on the abscissa refer to scaling factors for the intermolecular distance at the equilibrium; that is, 1.0 refers to the equilibrium, 0.90 and 0.95 to two shorter, and 1.05−2.00 to five larger distances of the monomers; see ref 38.

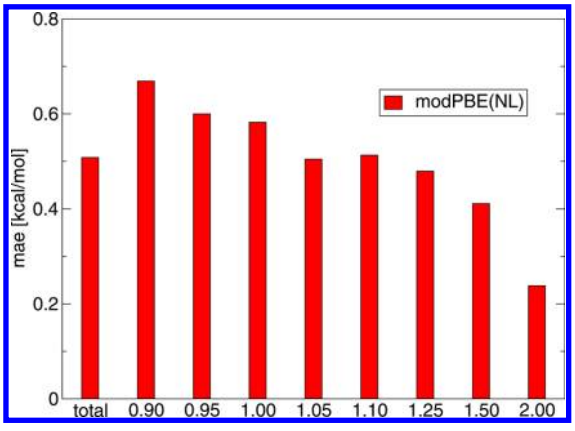

Figure 2. IonHB database: mean absolute errors of modPBE(NL) interaction energies to extrapolated CCSD(T) values. The numbers on the abscissa refer to scaling factors for the intermolecular distance at the equilibrium; that is, 1.0 refers to the equilibrium, 0.90 and 0.95 to two shorter, and 1.05−2.00 to five larger distances of the monomers; see ref 39.

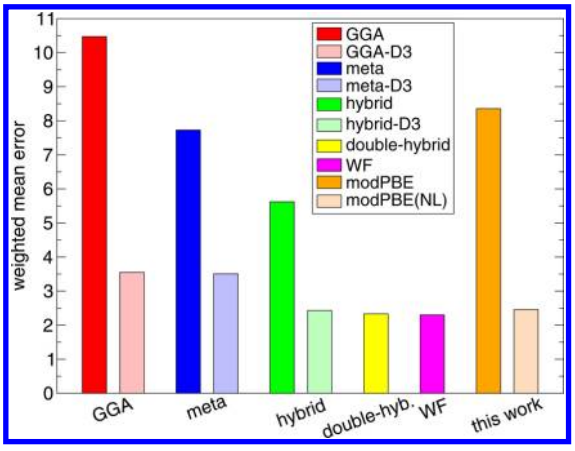

Figure 3. GMTKN30 database (14 subsets): weighted mean absolute errors of several density functional theory methods (in- and excluding dispersion corrections) and wave function methods (WF) to accurate reference results for the 14 chosen subsets.

coefficients describing the long-range interaction energy between two molecules depend on the chemical environment. In particular, atom−atom contributions to the dispersion energy calculated from localized polarizabilities depend on the hybridization or oxidation state of the contributing atoms.[55,56] A recent work by Johnson has analyzed this dependency for the dispersion coefficients from the XDM model.[57] In comparison to the XDM model, standard DFT+D methods are unable to account for the hybridization state of the atoms because of the nonlocal origin of this property. Thus, a number of DFT+D methods have been developed that try to capture these effects using different techniques.[18,20,22]

dx.doi.org/10.1021/ct300735g | J. Chem. Theory Comput. XXXX, XXX, XXX−XXX

Since the nonlocal correlation contribution to the energy in the NLDFT method explicitly depends on the electron density (see eq 3), it can be expected that it will also to some extent depend on the hybridization or oxidation state of the underlying atoms. In contrast to explicit dispersion corrections, however, the asymptotic behavior of the atom−atom contributions to the correlation energy in the NLDFT approach can not be directly calculated but has to be estimated from the form of the interaction energy curve of the two atoms. In Figure 4, the (absolute value of the) interaction energy

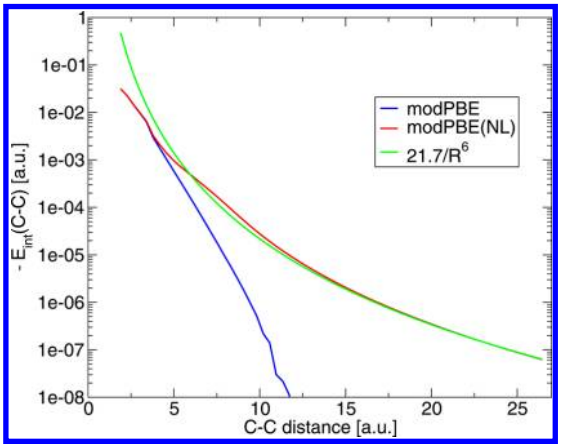

Figure 4. Interaction energy contribution of two carbon atoms located on different monomers in the stacked structure of the ethyne dimer.

contribution of two carbon atoms located on different monomers in the stacked structure of the ethyne dimer is shown for both the uncorrected and the corrected modPBE functional. It can be observed that for small distances of the two atoms both functionals yield the same C−C interaction energy contribution while at about 4.5 bohr the interaction energy curves of both methods start to differ. In case of modPBE, as expected, an exponential decrease of the C−C interaction contribution is observed while the modPBE(NL) interaction energy curve asymptotically decays as $\sim -1/R^6$. This shows that atomic C_6 dispersion coefficients can well be estimated from the asymtotic behavior of the atom−atom interaction energy contributions.

To analyze the dependence of the atomic C_6 dispersion coefficients, extracted from the energy decomposition of the NLDFT dimer correlation energy, on the hybridization state of carbon, the same set of carbon hydride molecules as in ref 57 has been used; see Table 3. For this, as in case of the ethyne dimer example described above, the atom−atom decomposition of the correlation energy of the dimer has been made for various distances of the two monomers and the interaction energy contributions for two carbon atoms was then fitted to the function $-C_6/R^6$ in the far asymptotic range of R(C−C) ≥ 20 bohr. It has been observed that the atomic C_6 coefficients calculated in this way are relatively insensitive with respect to the relative orientation of the two monomers. For example, in case of the ethyne dimer the estimated C_6(C−C) coefficient calculated from a linear configuration of the ethyne molecules is only about 0.2 au larger than for a stacked configuration. This shows that the NLDFT correction, as most other dispersion corrections to DFT functionals, is not able to describe the anisotropy of the long-range correlation energy quantitatively correctly, since as a result of the larger polarizabilty of the ethyne molecule along the molecular axis compared to

Table 3. Estimated Atomic C_6 Dispersion of Carbon in Various Compounds (in au)[a]

monomer	modPBE(NL)	XDM
C	29.6	41.9
$(CH_3)_3C^-$	24.4	29.9
C_2H_2	21.7	25.0
C_2H_4	20.2	20.9
C_6H_6	19.6	19.0
C_2H_6	18.8	17.8
$(CH_3)_3C\bullet$	19.1	17.6
coronene	18.9	16.8
$(CH_3)_3CH$	18.9	16.1
$(CH_3)_3C^+$	18.0	14.6

[a]For cases where distinct carbon atoms are present, the values refer to the central carbon atom. For comparison the last column contains the XDM (exchange-hole dipole moment) dispersion coefficients of ref 57.

perpendicular directions one can expect that also the dispersion energy is larger in the linear configuration of the molecules. In the following examples, the monomers were oriented such that the main axis of rotation was set parallel to each other with exception of $(C_6H_6)_2$ and $(\text{coronene})_2$ for which a stacked structure has been chosen, respectively.

As can be observed in Table 3, the C_6(C−C) values of modPBE(NL) clearly depend on the underlying hybridization of the carbon atoms, ranging from 29.6 au in the "electron rich" single carbon atom to 18.0 au in $(CH_3)_3C^+$. A comparison to the XDM dispersion coefficients of Johnson[57] shows, however, that this dependency is less strong than with the XDM model. For example, in the case of the $(CH_3)_3C^-$ anion, the XDM dispersion coefficient for the central carbon atom is about 5 au larger while in case of the $(CH_3)_3C^+$ cation it is 3.4 au smaller. The order of the compounds regarding the magnitude of the C_6(C−C) values is, aside from few exceptions, the same for NLDFT and XDM with the general trend that the carbon−carbon interaction decreases in the order of the hybridization $sp > sp^2 > sp^3$.

Table 4 displays atomic C_6 dispersion coefficients of nitrogen and phosphorus in different oxidation states. Again, it can be seen that the NLDFT coefficients depend less strongly on the environment than the XDM coefficients. Both the NLDFT and the XDM atomic dispersion coefficients vary with the oxidation

Table 4. Estimated Atomic C_6 Dispersion of Nitrogen and Phosphorus in Various Compounds (in au)[a]

monomer	modPBE(NL)	XDM
N	21.0	25.8
N_2	14.7	19.3
NO	17.2	21.8
NO_2	14.1	16.2
NO_3	13.2	13.4
N_2O_4	14.2	13.8
P	44.6	161
P_4	39.1	112
PO	37.6	130
PO_2	30.5	97
PO_3	27.3	82
P_4O_{10}	28.3	75

[a]The XDM dispersion coefficients of Johnson[57] are displayed for comparison.

dx.doi.org/10.1021/ct300735g | J. Chem. Theory Comput. XXXX, XXX, XXX−XXX

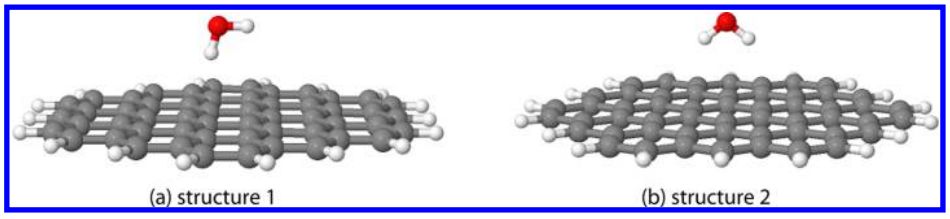

Figure 5. Water−acene geometries, see refs 45 and 46 for details.

Table 5. Water−Acene Interaction Energies from modPBE(NL) (in kcal/mol)[a]

	structure 1			structure 2		
acene	def2-SVP	def2-TZVP	def2-QZVP	def2-SVP	def2-TZVP	def2-QZVP
C_6H_6	−2.744	−3.216	−3.105	−3.229	−3.437	−3.285
$C_{24}H_{12}$	−2.739	−2.845	−2.864	−3.515	−3.372	−3.357
$C_{54}H_{18}$	−2.653	−2.821	−2.838	−3.357	−3.241	−3.2345
$C_{96}H_{24}$	−2.557	−2.764		−3.239	−3.161	
$C_{150}H_{48}$	−2.501			−3.147		
graphene		−2.659			−2.867	

[a]The estimated water−graphene interaction energies are calculated using the difference of the noncharge penetration electrostatic interaction energies as well as the nonlocal correlation contributions of DBC−H_2O and graphene−H_2O, as described in the text.

Table 6. Nonlocal Correlation Contribution to the Water−Acene Interaction Energies from modPBE(NL) (in kcal/mol)

	structure 1			structure 2		
acene	def2-SVP	def2-TZVP	def2-QZVP	def2-SVP	def2-TZVP	def2-QZVP
C_6H_6	−1.848	−1.917	−1.930	−1.733	−1.805	−1.821
$C_{24}H_{12}$	−2.772	−2.865	−2.871	−2.550	−2.650	−2.655
$C_{54}H_{18}$	−2.906	−3.002	−3.007	−2.689	−2.794	−2.798
$C_{96}H_{24}$	−2.934	−3.030		−2.717	−2.823	
$C_{150}H_{48}$	−2.940			−2.721		
graphene	−2.941	−3.037		−2.723	−2.830	

number of the N/P atom, being larger for the compounds in which the N/P atom has a small oxidation number and smaller for the compounds in which the N/P atom has a high oxidation number. However, while in the case of the nitrogen compounds the C_6 dispersion coefficients of NLDFT and XDM are of the same order, Table 4 shows that for phosphorus the NLDFT dispersion coefficients are smaller by a factor of 4 compared to the XDM ones. Taking into account that compared to the XDM dispersion coefficients the dispersion coefficients of phosphorus calculated by the D3 correction of Grimme[20] are even larger,[57] it can be concluded that the asymptotic behavior of the P−P interaction is considerably underestimated in the NLDFT method. This can be explained by the fact that the same parameters p_1 and p_2 were used for N and P in the modified density function, eq 8, which yielded interaction energies of nitrogen and phosphorus hydride dimers at equilibrium distances with similar accuracy. A more rigorous fitting procedure therefore would also include dimers at larger monomer distances.

4.4. Estimation of Water−Graphene Interaction Energy. The interaction energy of a water molecule with a graphene surface is estimated by using cluster models of water with acenes with increasing size. The two geometries considered for this study are shown in Figure 5 and are taken from refs 45 and 46. These correspond to the two possible OH−π structures, in which either only one (structure 1) or both hydrogen atoms (structure 2) interact with the π-system. While the true minimum structures of the modPBE(NL) method for these two cases are likely displaced from the geometries used in refs 45 and 46, scans of the potential energy surface have revealed that it is relatively flat for both structures[46] and an uncertainty of about ±0.15 kcal/mol can be anticipated in both cases.

The total interaction energies of H_2O with acene molecules containing 6, 24, 54, 96, and 150 atoms calculated with various basis sets (def2-XVP, x = S,T,Q) are shown in Table 5. In concordance with the studies of refs 45 and 46, it is found that the second structure is energetically more favorable compared to structure 1, for the $C_{96}H_{24}$−H_2O dimer the energy difference amounts to about 0.4 kcal/mol (def2-TZVP basis set), which agrees well with the findings of ref 46. A comparison of the interaction energies for a given dimer and structure calculated with differing basis sets shows that the def2-SVP results are not yet converged to an accuracy of 0.1 kcal/mol while in case of the def2-TZVP results the interaction energies deviate only by about 0.02 kcal/mol from the interaction energies using the def2-QZVP basis set (with exception of the benzene−H_2O dimer, in which the deviation is larger in magnitude for both structures). Therefore, the def2-TZVP results are accurate enough for an extrapolation to the graphene−water limit.

However, as can be observed in Table 1, the interaction energy for the $C_{96}H_{24}$−H_2O dimer is not yet well converged with respect to the cluster size, indicated by the still significant decrease in the interaction energy from $C_{54}H_{18}$−H_2O to $C_{96}H_{24}$−H_2O. As analyzed by using intermolecular perturbation theory in ref 45, the main contributions to the interaction energy between water and acenes that depend strongly on the size of the surface are the (noncharge-penetration contribution

dx.doi.org/10.1021/ct300735g | J. Chem. Theory Comput. XXXX, XXX, XXX−XXX

to the) electrostatic interaction energy and the dispersion energy. All other contributions, namely first-order exchange, second-order induction, and second- and higher order exchange contributions, are already well converged for the $C_{54}H_{18}$–H_2O dimer. This also holds true for the charge-penetration contribution to the electrostatic interaction due to the exponential decay of the overlap of the densities of the two monomers. Therefore, to be able to extrapolate the results to the graphene–H_2O case, here the nonlocal correlation contribution and the multipole–multipole contribution to the electrostatic interaction energy have been separately extrapolated and the resulting energy differences ($E_{surface} - E_{cluster}$) were then added to the total interaction energy for the $C_{96}H_{24}$–H_2O dimer.

Table 6 contains the nonlocal correlation contributions to the interaction energies for the various water–acene dimers for the modPBE(NL) functional calculated from the difference of the modPBE(NL) and modPBE correlation energies (eqs 3 and 6, note that the modPBE correlation energies were calculated by using the modPBE(NL) densities). As can be observed, in contrast to the total interaction energies shown in Table 6, the nonlocal contributions to the correlation energy are well converged already in case of the $C_{96}H_{24}$–H_2O dimer. The extrapolation of the nonlocal correlation contributions using an exponential function lead to a decrease of only 7 mkcal/mol for both structures (def2-TZVP basis set). The reason for this fast convergence of the nonlocal correlation contribution with increasing size of the acene molecules lies in the comparably fast decay of $1/R_{AB}^6$ of the correlation contribution of two interacting atoms A and B in the modPBE(NL) functional; see section 2.

In contrast to this, the asymptotic contribution to the electrostatic interaction energy for the water–acene dimers decays as $1/R^4$ (dipole–quadrupole) and $1/R^5$ (quadrupole–quadrupole) with increasing distance R of the monomers and therefore is expected to converge more slowly with the size of the acene system. (Note also in this context that in smaller acene–water dimers there will be undesired nonzero interaction contributions between the water molecule and the hydrogen atoms of the acene molecule that is one of the disadvantages using the cluster model.) In this work, the asymptotic (i.e., multipole–multipole or noncharge-penetration) contribution to the electrostatic interaction energy between water and acene molecules has been calculated from the distributed multipoles of the two monomers with a rank up to $l = 5$ using the modPBE densities; see section 3 for more details. The results are displayed in Table 7. One can see that in case of both structures there is still a significant decrease of the electrostatic interaction energy from the $C_{54}H_{18}$–H_2O to the $C_{96}H_{24}$–H_2O dimer, which complicates an extrapolation to the graphene–water case. However, as has been found by Jenness and Jordan (JJ),[45] the distributed multipoles of the inner carbon atoms of the acene systems are practically the same for coronene and DBC; that is, they can be used to approximate the distributed multipoles of carbon for graphene with good accuracy. Thus, in refs 45 and 46 the electrostatic interaction energy has been extrapolated by using a finite, yet large cluster, namely $C_{216}H_{36}$–H_2O and assigning only the estimated $Q20$ moments to the carbon atoms. In this work, principally, the same approach is used. However, here also, all nonvanishing (at an infinite size of the surface) multipoles up to rank $l = 5$ on the carbon atom were taken from the inner carbon atoms of the $C_{96}H_{24}$ molecules. These were $Q20 = -1.150$, $Q33s = -1.150$, $Q40 = -2.273$, and $Q53s = -5.105$ (values in au, orientation of the molecules described in section 3). The electrostatic interaction energy was then calculated using a periodic lattice of the graphene surface and adding an Ewald summation correction to the electrostatic energy calculated in real-space (as implemented in the Orient program[47]). The results for the electrostatic interaction energies for both structures are shown in Table 7. One can see that the multipole–multipole part of the electrostatic interaction energy almost vanishes at an infinite graphene sheet; in the case of structure 1, even a small positive electrostatic interaction energy is obtained. Referring to structure 1, this finding is basically the same as has been made also by JJ, see ref [45]. However, in case of structure 2 JJ obtained an estimate of −0.65 kcal/mol for the total multipole interaction energy between water and graphene which deviates strongly from the value of this work. Moreover, with exception of the benzene–water dimer, for which the multipole–multipole interaction energy is identical to within 3 millihartree (see Table 7 from this work and Table 5 from ref 46) for the larger acene–water dimers, the multipole–multipole interaction energies reported by JJ are significantly larger on magnitude (coronene–water: +0.32 kcal/mol. DBC–water: +0.33 kcal/mol) than the results of this work. Possible sources for this deviation are the somewhat larger quadrupole moments for carbon atoms (calculated from MP2/cc-pVDZ densities) used in ref 46 and the different multipoles used for the water molecule (JJ used Dang-Chang charges[58] on the water atoms).

Using the differences between the respective energy contributions for the $C_{96}H_{24}$–H_2O and the extrapolated graphene–H_2O system from Tables 6 and 7, the total interaction energies for the acene–water dimers were then extrapolated to the graphene–water case, yielding −2.66 kcal/mol for structure 1 and −2.87 kcal/mol for structure 2. In the case of structure 1, this estimate is almost 0.5 kcal/mol lower than the DFT-SAPT value obtained by JJ[45] while for the second structure the predicted interaction energy agrees well with the one reported by JJ and also with other theoretical estimates that lie in the range from −2.56 to −3.54 kcal/mol; see refs 46 and 59–63.

Table 7. Electrostatic (Multipole–Multipole) Interaction Energies of Water–Acene Dimers Using the Distributed Multipoles Calculated from modPBE Densities (def2-TZVP Basis Set, Energies in kcal/mol)

acene	structure 1	structure 2
C_6H_6	−1.988	−1.803
$C_{24}H_{12}$	−0.415	−0.784
$C_{54}H_{18}$	−0.227	−0.443
$C_{96}H_{24}$	−0.122	−0.301
graphene	0.018	-2.6×10^{-4}

5. SUMMARY

A direct correction approach (termed as NL correction hereafter) to (semi)local density-functional theory (DFT) methods has been implemented and tested, which enables the description of nonlocal correlation effects within DFT. The method is based on an atom–atom decomposition of the correlation energy density of the PBE correlation functional via a double Hirshfeld-type partitioning of the molecular volume. By this the atom–atom contributions to the total correlation energy could then be corrected through atomic weight

dx.doi.org/10.1021/ct300735g | J. Chem. Theory Comput. XXXX, XXX, XXX–XXX

functions that decay only as $1/R^6$ in contrast to exponentially decaying atomic densities, thus leading to a qualitatively correct description of the interaction contribution to the correlation energy for spatially separated molecules. In contrast to existing explicit dispersion corrections to DFT methods that are based on adding damped atom−atom dispersion correction terms to the total DFT energy (DFT+D methods), the approach used in this work also affects the Kohn−Sham orbitals and eigenvalues and is thus more akin to so-called van der Waals functionals[11,15] or meta-GGA functionals that are parametrized to describe long-range interactions.[3,6] On the other hand, however, the NL correction uses empirical atomic parameters for the weight functions that were determined by reproducing the CCSD(T) interaction energies of hydrogen-bonded dimers. Because of this, the NL correction cannot be regarded as a rigorous extension to standard DFT and, furthermore, in contrast to DFT+D methods, lacks a physical interpretation of the underlying atomic parameters used.

The test of the modPBE(NL) functional on a number of benchmark databases has shown, however, that it yields intermolecular interaction energies with a high accuracy: for the S22[16] and S66 × 8[38] benchmark databases of Hobza, mean errors of only 0.2 kcal/mol are obtained on average at the equilibrium structures. This is much better than with most other DFT+D methods[23,41,42] and also other DFT methods that aim at describing van-der-Waals interactions.[13,15] However, as was found for the IonHB database of Hobza et al.,[39] this accuracy deteriorates significantly for describing the interaction energies of dimers containing charged molecules. Though not analyzed in this work, this likely does not stem from an inaccurate description of the correlation contribution but the charge-transfer (part of the induction) contribution to the interaction energy and would be improved by including also nonlocal exchange contributions (as in hybrid functionals) in the xc functional.

The modPBE(NL) functional was also tested for a subset of 14 databases from the GMTKN30 database of Grimme et al.,[41,42] containing, in addition to databases for inter- and intramolecular dispersion interactions, also databases for thermochemical and kinetic properties of molecular systems containing main-group elements. An overall error analysis for this study has shown that the NL correction not only clearly improves the performance of the corresponding noncorrected standard modPBE functional, but the average error is also clearly smaller than commonly with GGA+D or meta-GGA+D methods yet comparable to hybrid- and double-hybrid-GGA functionals with the D3 correction of Grimme.[20] Therefore, the modPBE(NL) functional might be useful also for studying properties other than intermolecular interaction energies.

Since the long-range correlation correction of the NLDFT method explicitly depends on the electron density, it has been analyzed to which extent atom−atom contributions vary with the hybridization or oxidation state of the underlying atoms using a set of small carbon, nitrogen, and phosphorus compounds. It could be demonstrated that the estimated atom−atom C_6 coefficients extracted from NLDFT interaction energies qualitatively correctly describe the decrease of the C_6 coefficient with larger hybridization state respectively larger oxidation number of the corresponding atoms. Thus, in contrast to DFT+D methods that use fixed atomic C_6 coefficients, the NLDFT correction is more capable to account for the dependence of the long-range correlations on the chemical environment. It has been found, however, that the atomic C_6 coefficients from the NLDFT method vary less strongly with the hybridization or oxidation state than corresponding C_6 coefficients from the XDM model.[57] Moreover, in the case of phosphorus, the magnitude of the NLDFT and XDM C_6 coefficients differed considerably, so that it can be expected that for dimer systems including phosphorus (or other third row elements) the interaction energy will not be accurate for larger monomer distances. A more sophisticated fitting procedure to determine the parameters in the density function of eq 8 therefore should include also dimers with larger monomer distances in the fitting set.

On account of the reasonable accuracy of the modPBE(NL) functional for reproducing intermolecular interaction energies, the method has also been tested for describing the interaction energy between a water molecule and a graphene surface. This has been done by using the cluster model of Feller and Jordan[64] in which the graphene surface is represented by acene molecules of larger and larger size so that the interaction energy for finite clusters can be extrapolated to the interaction energy of water with an infinite graphene sheet. It has been found, however, that a direct extrapolation of the total interaction energy is difficult due to the slowly converging noncharge-penetration contributions to the electrostatic interaction energy. A separate extrapolation of this interaction contribution and the nonlocal correlation contribution yielded total interaction energies of −2.7 and −2.9 kcal/mol for the single hydrogen-bridged and the double hydrogen-bridged structure. While the former value is found to be significantly lower by 0.5 kcal/mol on magnitude than a previous theoretical estimate using the DFT-SAPT method,[45] the second value corresponding to the global minimum structure compares well with the predictions of other theoretical methods that are clustered around −3.0 kcal/mol; see refs 46 and 59−63.

In summary, the nonlocal correction scheme to DFT functionals developed and tested in this work is found to lead to clear improvements for describing long-range interactions as well as thermochemical and kinetic properties of large and medium sized molecules compared to standard DFT. It might therefore be useful as an alternative method to commonly applied DFT+D methods for the description of molecular systems in which the account for long-range interactions is important.

■ ASSOCIATED CONTENT

Supporting Information

Diagrams containing mean absolute errors of the NLDFT method to accurate reference results for the 14 subsets of the GMTKN30 database as well as tables containing all energy values. This information is available free of charge via the Internet at http://pubs.acs.org/.

■ AUTHOR INFORMATION

Corresponding Author

*E-mail: andreas.hesselmann@chemie.uni-erlangen.de.

Notes

The authors declare no competing financial interest.

■ REFERENCES

(1) Parr, R. G.; Yang,W. *Density-Functional Theory of Atoms and Molecules*; Oxford University Press: Oxford, 1989.

(2) Please refer to the recent review: Grimme, S. Density functional theory with London dispersion corrections. *Rev.: Comp. Mol. Sci.* **2011**,

1, 211 which gives a good overview of the different DFT methods that are corrected to include long-range correlation interactions.
(3) Zhao, Y.; Schultz, N. E.; Truhlar, D. G. *J. Chem. Phys.* **2006**, *2*, 364.
(4) Zhao, Y.; Truhlar, D. G. *J. Chem. Phys.* **2006**, *125*, 194101.
(5) Zhao, Y.; Truhlar, D. G. *J. Phys. Chem.* **2006**, *110*, 13126.
(6) Zhao, Y.; Truhlar, D. G. *J. Chem. Theory Comput.* **2008**, *4*, 1849.
(7) Zhao, Y.; Truhlar, D. G. *Theor. Chem. Acc.* **2008**, *120*, 215.
(8) Hohenstein, E. G.; Chill, S. T.; Sherrill, C. D. *J. Chem. Theory Comput.* **2008**, *4*, 1996.
(9) Johnson, E. R.; Becke, A. D.; Sherrill, C. D.; DiLabio, G. A. *J. Chem. Phys.* **2009**, *131*, 034111.
(10) Andersson, Y.; Langreth, D. C.; Lundqvist, B. I. *Phys. Rev. Lett.* **1996**, *76*, 102.
(11) Dion, M.; Rydberg, H.; Schröder, E.; Langreth, D. C.; Lundqvist, B. I. *Phys. Rev. Lett.* **2004**, *92*, 246401.
(12) Langreth, D. C.; Dion, M.; Rydberg, H.; Schröder, E.; Hylgaard, P.; Lundqvist, B. I. *Int. J. Quantum Chem.* **2005**, *101*, 599.
(13) Vydrov, O. A.; Van Voorhis, T. *Phys. Rev. Lett.* **2009**, *103*, 063004.
(14) Vydrov, O. A.; Van Voorhis, T. *J. Chem. Phys.* **2010**, *132*, 164113.
(15) Vydrov, O. A.; Van Voorhis, T. *J. Chem. Phys.* **2010**, *133*, 244103.
(16) Jurečka, P.; Šponer, J.; Černý, J.; Hobza, P. *Phys. Chem. Chem. Phys.* **2006**, *8*, 1985.
(17) Elstner, M.; Hobza, P.; Frauenheim, T.; Suhai, S.; Kaxiras, E. *J. Chem. Phys.* **2001**, *114*, 5149.
(18) Wu, Q.; Yang, W. *J. Chem. Phys.* **2002**, *116*, 515.
(19) Grimme, S. *J. Comput. Chem.* **2006**, *27*, 1787.
(20) Grimme, S.; Antony, J.; Ehrlich, S.; Krieg, H. *J. Chem. Phys.* **2010**, *132*, 154104.
(21) Grimme, S. *J. Comput. Chem.* **2004**, *25*, 1463.
(22) Tkatchenko, A.; Scheffler, M. *Phys. Rev. Lett.* **2009**, *102*, 073005.
(23) Marom, N.; Tkatchenko, A.; Rossi, M.; Gobre, V. V.; Hod, O.; Scheffler, M.; Kronik, L. *J. Chem. Theory Comput.* **2011**, *7*, 3944.
(24) Sato, T.; Nakai, H. *J. Chem. Phys.* **2009**, *131*, 224104.
(25) Becke, A. D.; Johnson, E. R. *J. Chem. Phys.* **2005**, *122*, 154104.
(26) Becke, A. D.; Johnson, E. R. *J. Chem. Phys.* **2005**, *123*, 024101.
(27) Becke, A. D.; Johnson, E. R. *J. Chem. Phys.* **2007**, *127*, 154108.
(28) Kong, J.; Gan, Z.; Proynov, E.; Freindorf, M.; Furlani, T. R. *Phys. Rev. A* **2009**, *79*, 042510.
(29) Steinmann, S. N.; Corminboeuf, C. *J. Chem. Phys.* **2011**, *134*, 044117.
(30) Heßelmann, A. *J. Chem. Phys.* **2012**, *136*, 014104.
(31) von Lilienfeld, O. A.; Tavernelli, I.; Röthlisberger, U.; Sebstiani, D. *Phys. Rev. Lett.* **2004**, *93*, 153004.
(32) von Lilienfeld, O. A.; Tavernelli, I.; Röthlisberger, U.; Sebastiani, D. *Phys. Rev. B* **2005**, *71*, 195119.
(33) Lin, I.; Röthlisberger, U. *Phys. Chem. Chem. Phys.* **2008**, *10*, 2730.
(34) Lin, I.; Coutinho-Neto, M. D.; Felsenheimer, C.; von Lilienfeld, O. A.; Röthlisberger, U. *Phys. Rev. B* **2007**, *75*, 205131.
(35) Tapavicza, E.; Lin, I.; von Lilienfeld, O. A.; Tavernelli, I.; Coutinho-Neto, M. D.; Röthlisberger, U. *J. Chem. Theory Comput.* **2007**, *3*, 1673.
(36) Leach, A. R. *Molecular Modelling: Principles and Applications*; AddisonWesley Publishing Company: Westchester, NY, 1997; p58.
(37) Perdew, J. P.; Burke, K.; Ernzerhof, M. *Phys. Rev. Lett.* **1996**, *77*, 3865.
(38) Rezak, J.; Riley, K. E.; Hobza, P. *J. Chem. Theory Comp.* **2011**, *7*, 2427.
(39) Rezak, J.; Hobza, P. *J. Chem. Theory Comput.* **2012**, *8*, 141.
(40) Goerigk, S.; Grimme, S. *Phys. Chem. Chem. Phys.* **2011**, *13*, 6670.
(41) Goerigk, S.; Grimme, S. *J. Chem. Theo. Comput.* **2011**, *7*, 291.
(42) Grimme, S. *GMTKN30—A Database for General Main Group Thermochemistry, Kinetics, and Noncovalent Interactions.* http://toc.unimuenster.de/GMTKN/GMTKN30/GMTKN30main.html (accessed Oct. 2012).
(43) Rezac, J.; Jurecka, P.; Riley, K. E.; Cerny, J.; Valdes, H.; nd K. Berka, K. P.; Rezac, T.; Pitonak, M.; Vondrasek, J.; Hobza, P. *Collect. Czech. Chem. Commun.* **2008**, *73*, 1261.
(44) Takatani, T.; Hohenstein, E. G.; Malagoli, M.; Marshall, M. S.; Sherrill, C. D. *J. Chem. Phys.* **2010**, *132*, 144104.
(45) Jenness, G. R.; Jordan, K. D. *J. Phys. Chem. C* **2009**, *113*, 10242.
(46) Jenness, G. R.; Karalti, O.; Jordan, K. D. *Phys. Chem. Chem. Phys.* **2010**, *12*, 6375.
(47) Stone, A. J.; Dullweber, A.; Engkvist, O.; Fraschini, E.; Hodges, M. P.; Meredith, A. W.; Nutt, D. R.; Popelier, P. L. A.; Wales, D. J. *Orient: A Program for Studying Interactions between Molecules*, version 4.7; University of Cambridge: Cambridge, 2010.
(48) Stone, A. J. *J. Chem. Theory Comput.* **2005**, *1*, 1128.
(49) Weigend, F.; Furche, F.; Ahlrichs, R. *J. Chem. Phys.* **2003**, *119*, 12753.
(50) Weigend, F.; Ahlrichs, R. *Phys. Chem. Chem. Phys.* **2005**, *7*, 3297.
(51) Weigend, F. *J. Comput. Chem.* **2008**, *29*, 167.
(52) Boys, S. F.; Bernadi, F. *Mol. Phys.* **1970**, *19*, 553.
(53) Werner, H.-J. et al. *MOLPRO*, version 2010.1, a package of ab initio programs; University College Cardiff Consultants Ltd.: Cardiff, U.K., 2010. Available online: http://www.molpro.net.
(54) L. Goerigk, H. K.; Grimme, S. *Chem. Phys. Chem.* **2011**, *12*, 3421.
(55) Lillestolen, T. C.; Wheatley, R. J. *J. Phys. Chem. A* **2007**, *111*, 11141.
(56) Wheatley, R. J.; Lillestolen, T. C. *Mol. Phys.* **2008**, *106*, 1545.
(57) Johnson, E. R. *J. Chem. Phys.* **2011**, *135*, 234109.
(58) Dand, L. X.; Chang, T.-M. *J. Chem. Phys.* **1997**, *106*, 8149.
(59) Rubes, M.; Nachtigall, P.; Vondrasek, J.; Bludsky, O. *J. Phys. Chem.* **2009**, *113*, 8412.
(60) Sudiarta, I. W.; Geldart, D. J. W. *J. Phys. Chem. A* **2006**, *110*, 10501.
(61) Huff, E. M.; Pulay, P. *Mol. Phys.* **2009**, *107*, 1197.
(62) Reyes, A.; Fomina, L.; Rumsh, L.; Fomine, S. *Int. J. Quantum Chem.* **2005**, *104*, 335.
(63) Cabaleiro-Lago, E. M.; Carranza-Garcia, J. A.; Rodriguez-Otero, J. *J. Chem. Phys.* **2005**, *104*, 335.
(64) Feller, D.; Jordan, K. D. *J. Chem. Phys.* **2000**, *104*, 9971.